Available online at: http://www.advancedscientificjournal.com
http://www.krishmapublication.com
IJMASRI, Vol. 4, issue 1, pp. 1026- 1030, Jan. -2024
https://doi.org/10.53633/ijmasri

INTERNATIONAL JOURNAL OF MULTIDISCIPLINARY ADVANCED SCIENTIFIC RESEARCH AND INNOVATION (IJMASRI)

ISSN: 2582-9130 IBI IMPACT FACTOR 1.5 DOI: 10.53633/IJMASRI

RESEARCH ARTICLE

SYNTHESIS AND CHARACTERIZATION OF THICKNESS-DEPENDENT $CD_{0.7}FE_{0.3}S$ THIN FILMS

Barote M A[1] Landge S O[2] and Suryawanshi R V[3]*
1,2,3 Department of Electronics, Azad Mahavidyalaya Ausa, Ta. Ausa, Dist. Latur- 413520, M.S., India

Abstract

The thickness dependent $Cd_{0.7}Fe_{0.3}S$ thin films are deposited by chemical bath deposition method. The thickness of the $Cd_{0.7}Fe_{0.3}S$ thin films is increased by depositing layer after layer. X-ray diffraction (XRD) patterns of the thickness dependent films showed that the material deposited is polycrystalline in nature. Few reflections such as (2 0 0), (2 0 1) and (2 2 0) corresponding to hexagonal phases of FeS are detected. The effect of film thickness on the microstructure of $Cd_{0.7}Fe_{0.3}S$ thin films was studied. No appreciable changes in stoichiometric ratio were observed with change in film thickness.

Keywords: Film thickness, XRD, EDAX, hexagonal, crystallite size

Introduction

The thickness of thin films has a profound impact on their optical, electrical, mechanical, magnetic, chemical, and thermal properties. These effects are widely exploited in various technological applications and industries, making precise control of thin film thickness a critical consideration. (Pandey *et al.,* 1991; Wada and Nishimatsu 1978). As the thickness of a thin film changes, its optical properties can shift dramatically. Thin film thickness can significantly impact electrical properties, such as conductivity and resistance. In some cases, very thin films can show different electronic behaviors compared to their bulk counterparts. As the film becomes thinner, quantum effects might come into play, leading to altered charge carrier mobility and quantum confinement effects. Thin films are also commonly used in microelectronics and integrated circuits, where controlling the film thickness is crucial for achieving desired electrical performance.

Thin films have a higher surface-to-volume ratio compared to bulk materials, leading to enhanced chemical reactivity. This increased reactivity can be advantageous in catalysis and sensor applications, where a higher surface area allows for more efficient interactions with reactants or analytes ((Hull *et al.,* 1953; Deshmukh and Sawant 1991; Lokhande and Bhosale 1990; Rajpure *et al.,* 1999; Mathew 2000).

2. Experimental Techniques

The $Cd_{0.7}Fe_{0.3}S$ thin films of different thicknesses were deposited onto the amorphous glass

©2024 by KRISHMA PUBLICATION

substrates by using the chemical bath deposition method. The electrode thickness was increased by repeating the number of depositions. Each time the layers were exposed to the fresh quantities of reactants. The layer surface was cleaned after every successive deposition by double distilled water. These deposited films were termed as T1, T2, T3, T4, T5, and T6. The thickness of the deposited samples was measured by gravimetric weight difference method.

The structural, morphological and compositional, optical electrical characterization of the $Cd_{0.7}Fe_{0.3}S$ thin films of various thicknesses was carried out by using various characterization techniques such as X-ray diffraction (XRD), scanning electron microscopy (SEM), and energy dispersion analysis by X-ray (EDAX).

3 Results and discussion

3.1 Thickness studies

The thickness of the $Cd_{0.7}Fe_{0.3}S$ thin films is increased by depositing layer after layer on the earlier films. It is seen that, initially, the thickness increased almost linearly with the number of depositions and then saturated. This behavior can be explained as follows. The kinetics of film growth suggests that growth of the film takes place either by ion by ion condensation or by adsorption of the colloidal particles from the solution (Deshmukh and Sawant 1991; Masumdar 2000). For the first layer, we observed thin, adherent, relatively uniform and specularly reflecting films, showing the film growth by an ion by ion condensation of the ions on the substrate surface. For successive depositions, the earlier layer provides enough nucleation centers and the film growth proceeds further. If the number of depositions is increased further, the rate of adsorption of the colloidal particles on the substrate surface ceases and the film thickness tends towards saturation ((Deshmukh and Sawant 1991; Masumdar 2000). Fig.1 shows the variation of film thickness with number of layer deposition for $Cd_{0.7}Fe_{0.3}S$ thin film. The terminal layer thickness of the $Cd_{0.7}Fe_{0.3}S$ thin films of various thicknesses was measured by gravimetric weight difference density method using sensitive microbalance. The thickness of $Cd_{0.7}Fe_{0.3}$ S thin films of various thicknesses is tabulated in Table 1.

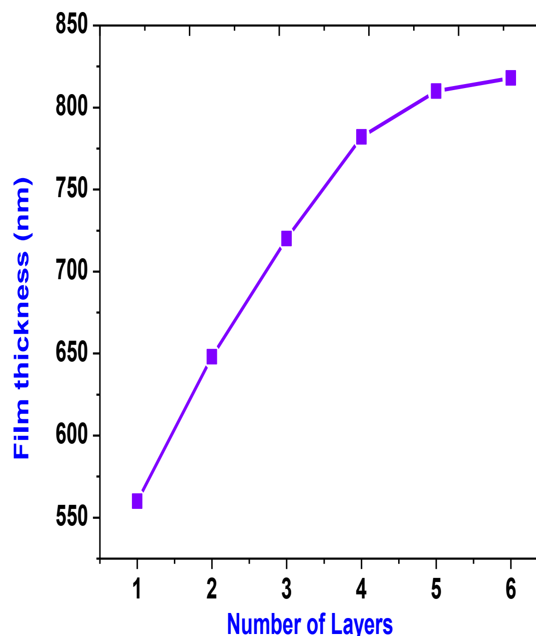

Fig. 1: Variation in thickness versus number of layers of $Cd_{0.7}Fe_{0.3}S$ thin films

3.2 X-ray diffraction (XRD) studies

Fig.2 shows the X-ray diffraction (XRD) patterns of the thickness dependent $Cd_{0.7}Fe_{0.3}S$ thin films. They show that the material deposited is polycrystalline in nature. The peaks were identified by comparing the 2θ-values obtained from the X-ray diffraction patterns with the standard JCPDS data-cards θ –values ((Rajpure *et al.,* 1999; Mathew 2000; Deshmukh and Sawant 1991; Masumdar 2000; Ma et al., 2007). From the diffractograms it is seen that the strongest diffraction peak for CdS is observed at 28.52^0, which can be indexed as (1 0 1) hexagonal. ((Amalnerkar *et al.,* 1985; Banerjee et al., 1984). However, the XRD patterns show additional peaks corresponding to distinctly hexagonal planes such as (1 0 0), (0 0 2), (1 1 0) and (1 1 2) plane for hexagonal phase. The results are similar to those reported by Amalnerkar *et al.,* 1985. Few reflections such as (2 0 0), (2 0 1) and (2 2 0) corresponding to hexagonal phases of FeS are detected. This indicates that the

©2024 by KRISHMA PUBLICATION

structure of $Cd_{0.7}Fe_{0.3}S$ thin films has hexagonal phases. Closer examination of the XRD patterns also reveals small peak of elemental Cd having very low intensities for thickness T1. The average grain size of the thin films was calculated for all the observed planes by using Scherrer's formula (Das and Damodare 1998).

$$D = \frac{k\lambda}{\beta \cos\theta} \quad (1)$$

where k varies from 0.89 to 1.39. But in most of the cases it is closer to 1. Hence for crystallite size calculation it is taken as 1, 'λ' is the wavelength of X-ray, 'β' is the full width of the peak maximum in radians and 'θ' is Bragg's angle. It is found that the average crystallite size increases with increasing thickness. Fig. 3 shows the variation of crystallite size versus layer thickness of film samples with different layers. From the XRD studies it is observed that with increasing the film thickness, the locations of the measured diffraction peaks do not change significantly but the intensities of the peaks increases. This is due to the crystallinity of the films being improved and crystallites becoming larger when elevating the film thickness. A similar behavior was observed by Oztas *et al., 2006*). Also XRD studies leads to the conclusion that crystallinity and degree of orientation of the $Cd_{0.7}Fe_{0.3}S$ thin films are closely related to the film thickne

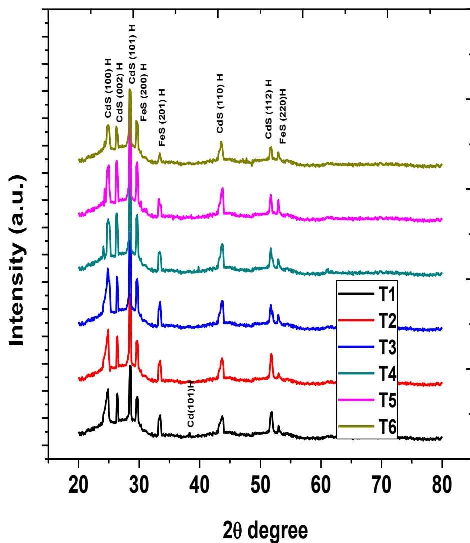

ss

Fig: 2. XRD patterns of $Cd_{0.7}Fe_{0.3}S$ thin films with various thicknesses.

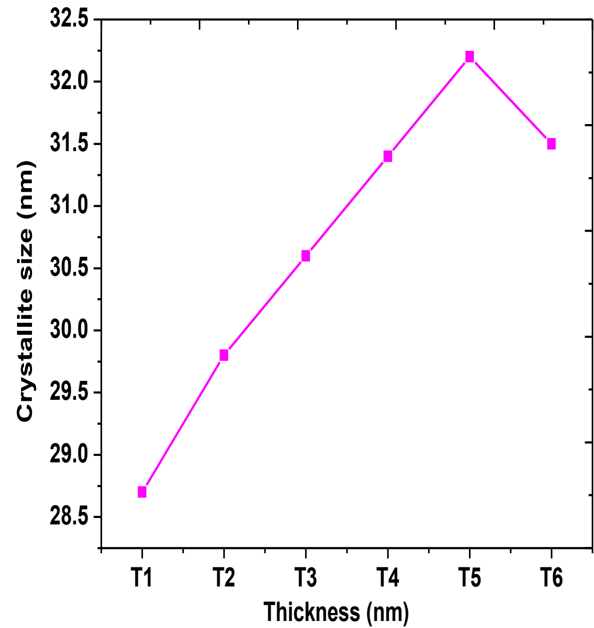

Fig. 3: Variation of crystallite size vs. thickness for $Cd_{0.7}Fe_{0.3}S$ thin films.

3.3 Scanning electron microscopy (SEM) studies

The effect of film thickness on the microstructure of $Cd_{0.7}Fe_{0.3}S$ thin films was studied from SEM images. Fig. 4 (a - c) shows the SEM images of samples T1, T3, and T5, respectively. From SEMs', it is seen that film formed are dense, smooth and homogeneous with well covered to the surface of the substrate without any visible holes. From the SEM micrographs, it is also seen that grain structure is improved with thickness. The average grain size of the micro-crystallites was calculated from intercept method as given by

$$\text{Average grain size} = \frac{1.5 \times l}{m \times n} \quad (2)$$

where m is the magnification of the micrograph, l is the length of the line drawn on the micrograph, n is the number of grains crossed by the line and 1.5 is the parameter assuming spherical grains. The calculated average grain sizes are tabulated in Table 1

©2024 by KRISHMA PUBLICATION

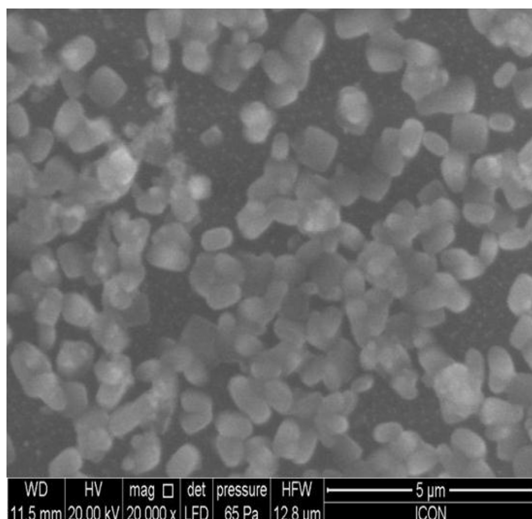

a) T1= 560nm

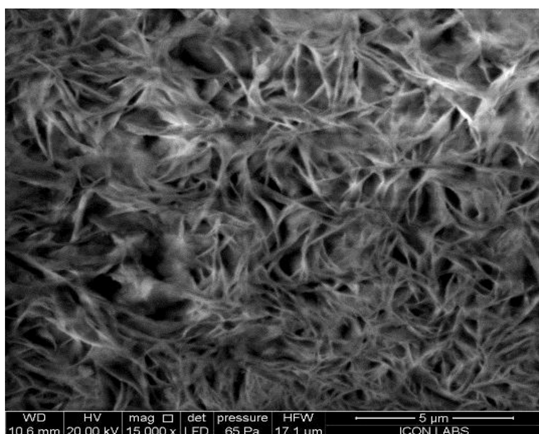

(c) T3= 720 nm

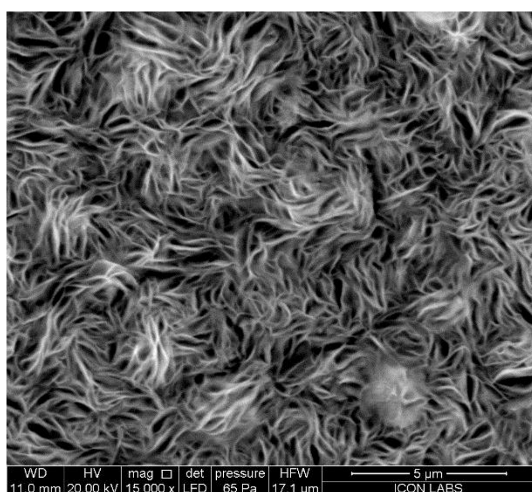

Fig. 4 (a-c): SEM of $Cd_{0.7}Fe_{0.3}S$ thin films with various thicknesses.

3.4 Energy dispersive analysis by X-ray (EDAX) studies

Fig. 5 shows an energy dispersive analysis (EDAX) pattern for a typical film thickness. It is seen that the atomic percentage of Cd in the films are greater while that for S is below expectation, resulting in sulpher deficient films. These stoichiometric deviations are responsible for n-type conduction of the films ((Deshmukh *et al.,* 1997; Gupta 1992; Kobayasi *et al.,* 2003; Yadav *et al.,* 2010). No appreciable changes in stoichiometric ratio were observed with change in film thickness. The details of relative analysis are given in Table 1.

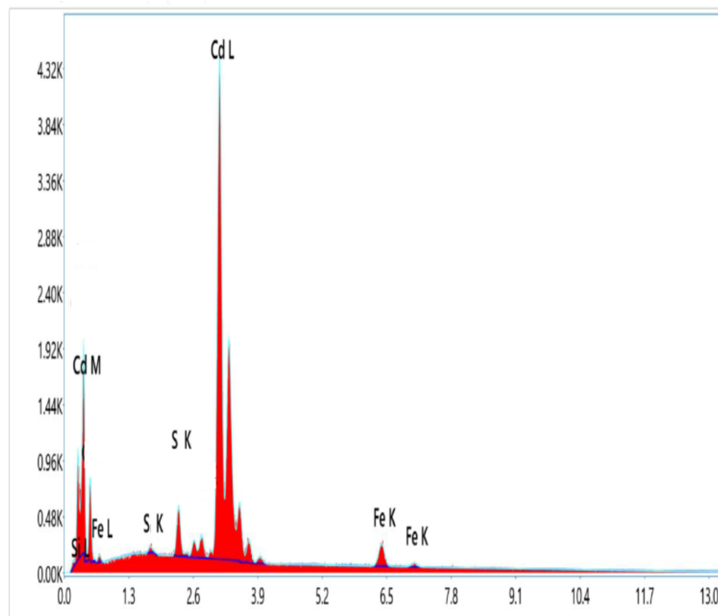

Fig. 5: Representative EDAX patterns of $Cd_{0.7}Fe_{0.3}S$ thin films

©2024 by KRISHMA PUBLICATION

Thickness µm	Grain size (nm) (SEM)	Elemental composition in film (%)		
		Cd	Fe	S
T1= 560 nm	231	52.02	8.30	39.68
T2= 648 nm	250	46.85	8.45	44.70
T3= 720 nm	264	47.92	8.25	43.82
T4= 782 nm	275	46.75	8.38	44.87
T5= 810 nm	288	45.88	8.41	45.71
T6= 828 nm	270	46.34	8.28	45.38

Table 1: EDAX analysis of $Cd_{0.7}Fe_{0.3}S$ thin films of various thicknesses

Conclusion

The thickness of the $Cd_{0.7}Fe_{0.3}S$ thin films increased almost linearly with the number of depositions and then saturated. From XRD it is seen that the strongest diffraction peak for CdS is observed at 28.52^0, which is indexed as (1 0 1) hexagonal. The structure of $Cd_{0.7}Fe_{0.3}S$ thin films has hexagonal phases. From SEM study, it is found that film formed are dense, smooth and homogeneous with well covered to the surface of the substrate. From EDAX it is seen that the films are sulpher deficient.

References

1. Pandey, R. K., Kumar, S. R and Rooz, A. J. N and Chandra, S. (1991). Thin Solid Film, 200 (1991) 1.
2. Wada, Y and Nishimatsu,S. (1978). J. Electrochem. Soc. 125 (1978) 1499.
3. Hull, F. C and Hork, W. J. (1953). J. Met. 5 (1953) 565.
4. Deshmukh, L. P and Sawant, V. S. (1991). Solar Cells, 31 (1991) 186.
5. Lokhande, C. D and Bhosale, C. H. (1990). Bull. Electrochem. 6 (1990) 622.
6. Rajpure, K. Y., Bamane, S. M. Lokhande, C. D and Bhosale, C. H. (1999). Ind. J.Pure Appl. Phys. 37 (1999) 413–420.
7. Mathew, X. (2000). J. Phys. D: Appl. Phys. 33 (2000) 1565–1571.
8. Deshmukh, L. P and Sawant, V. S. (1991). Solar Cells, 31 (1991) 186.
9. Masumdar, E. U. (2000). Ph. D. Thesis, Shivaji University, Kolhapur, India, (2000) p-192.
10. JCPDS data card no. 06-0314.
11. JCPDS data card no. 80-1028.
12. Ma, R. M., Dai, L. Huo, H.P. Xu, W. J and Qin, G. G. (2007). Nano Lett. 73 (2007) 300.
13. Wu, X. Y., Shen, D. Z. Zhang, Z. Z. Zhang, J. Y. Liu, K. W. Li, B. H. Lu, Y. M. Zhao, D. X and Yao, B. (2006). Appl. Phys. Lett. 89 (2006) 262118.
14. Amalnerkar, D. P., Pavaskar, N. R. Date, S. K and Sinha, A. P. B. (1985) Ind. J. Pure Appl. Phys. 23 (1985) 539.
15. Banerjee, R., Ray, S and Barua, A. K. (1984). Ind. J. Phys. 58A (1984) 166.
16. Das, V. D and Damodare, L. (1998). Mater. Chem. Phys. 56 (1998) 48.
17. Oztas, M., Bedir, M. Yazici, A. N. Kafadar, E. V. Toktamis, H. (2006). Physica B 381 (2006) 40.
18. Yadav, A. A., Barote, M. A. and Masumdar, E. U. (2010). Solid State Sci. 12 (2010) 1173.
19. Deshmukh, L. P., Shahane, G. S. Sutrave, D. S and Hankare, P. P. (1997). Solid State Phenomena 55 (1997) 68.
20. Gupta, T. K. (1992). J. Doh, Sol. Ener. Mater. Sol. Cells 27 (1992) 327.
21. Kobayasi, S., Takenobu, T. Mori, S. Fujiwara, A and Iwasa, Y. (2003). Appl. Phys. Letts. 82 (2003) 581

*****